Quantifying the Influence of Surface Roughness on Concrete Overlay Bonding in Sulfuric Acid Environments

Nurdeen Mohamed Altwair*, Younis Omran Yacoub, Alhussin Faraj Aliwan, Waled Faraj Alnaas, Saleh Elmahdi Abdulsalam, Abdualhamid Mohamed Alsharif

Department of Civil Engineering, El-Mergib University, Al-Khums, Libya

Received 06 January 2025; received in revised form 11 April 2025; accepted 15 April 2025

DOI: https://doi.org/10.46604/peti.2024.14713

Abstract

This study examines the impact of sulfuric acid on the concrete bond interface, emphasizing surface roughness variation. Three surface treatments: control surface (CS) defined as as-cast without surface preparation, drilled holes (DS), and grooved surfaces (GS). Specimens are immersed in a 5% sulfuric acid solution for 15 and 30 days. Bond performance is assessed through slant shear tests, splitting tensile tests, ultrasonic pulse velocity (UPV) measurements, mass loss evaluation, X-ray diffraction (XRD) analysis, and visual inspections of the degraded specimens. The results show that DS and GS significantly enhance shear and splitting tensile strength compared to CS. Among the treatments, GS specimens exhibited the highest shear strength and superior resistance to debonding under sulfuric acid exposure. While sulfuric acid exposure had minimal impact on UPV, roughened surfaces maintained higher UPV due to improved contact area. Visually, the GS specimens retained structural integrity after 30 days in 5% sulfuric acid, outperforming DS and CS specimens, as corroborated by XRD analysis.

Keywords: sulfuric acid, surface roughness, bonding strength, mass loss, UPV

1. Introduction

Concrete structure rehabilitation requires an in-depth understanding of the bond characteristics between new overlays and existing substrates. Recent advancements in structural engineering have significantly improved this knowledge, yet the interface bond strength remains a critical weakness, raising durability concerns and compromising structural integrity [1]. As the need for sustainable long-term use of existing facilities grows, structural health monitoring and damage detection have become crucial. Sensors implemented in industry enhance rehabilitation effectiveness and ensure long-term structural sustainability [2]. Integrating these modern techniques with comprehensive bond comprehension can reinforce rehabilitated concrete structures' safety and continued serviceability.

Surface roughening of existing concrete is crucial for successful new concrete bonding in structural reinforcement. Mechanical methods, such as scarifying, grinding, or shot blasting, effectively roughen the surface by removing the top layer and exposing aggregate. These methods enhance adhesion by increasing surface area and promoting mechanical interlocking. Various techniques, including steel brushing, chipping, drilling, sandblasting, water blasting, grinding, and grooving, have been studied to improve interfacial bond strength [3-5].

Deterioration at the interface between new and existing concrete can severely compromise structural integrity [5]. Environmental factors such as chlorides, acids, carbonation, freeze-thaw cycles, and temperature/humidity variations can induce cracking, ultimately leading to structural failure [6]. Chloride ingress is particularly problematic at new-to-old concrete

*Corresponding author. E-mail address: nmaltwair@elmergib.edu.ly

interfaces, especially in coastal or de-icing salt-exposed regions, as it accelerates reinforcement corrosion and threatens structural stability [6-7]. A substantial body of literature has focused on the resistance of these interfaces to chloride ion penetration. Li et al. [8] found that monolithic concrete exhibits superior chloride resistance compared to wet joints, irrespective of surface roughness. Furthermore, Li et al. [9] identified an "interfacial zone effect" (IZE), where moderate surface roughness minimizes chloride permeability. Qin et al. [10] demonstrated that shrinkage-reducing admixtures (SRAs) effectively reduce chloride penetration by lowering water diffusion.

Zhao et al. [11] combined their revised chloride diffusion model for precast prestressed bridge joints under fatigue loading with surface roughness analysis, revealing that increased roughness initially elevates but later decreases chloride concentrations within the interfacial zone under fatigue stress, while Xia et al. [12] linked higher porosity and microcrack formation at the interface, enriched in $CaCO_3$ precipitation, to increased chloride penetration. Zhang et al. [13] examined the influence of factors such as water-to-cement ratio and casting interval on bonding and chloride migration, finding significant differences in migration coefficients between interfaces and new/old concrete. Additionally, Gao et al. [14] investigated the effects of sulfate attack, revealing that roughened substrates exhibit superior corrosion resistance. Li et al. [15] studied carbonation resistance, finding monolithic concrete to be more resistant than various joint types. Lastly, Yi et al. [16] reported that rough substrate surfaces enhance freeze-thaw resistance, though improvements are limited to an optimal level of surface fractal dimension.

Concrete's high alkalinity (pH > 12) makes it vulnerable to acid deterioration from various sources, including moisture, combusted sulfurous gases in fuels, peat and clay soils, oxidation of sulfide minerals, anaerobic bacteria in sewage systems, rainfall, industrial water, and agricultural/food industry effluents [17]. These acids can deteriorate concrete structures through reactions with other chemicals, forming substances like acetic, lactic, oxalic, or citric acids. Concrete facilities used for waste treatment in agricultural and food industries are particularly susceptible to this type of deterioration. Acidic solutions can negatively impact the bonding between new and old concrete. When an acidic solution comes into contact with the interfacial transition zone (ITZ) between the overlay concrete and existing concrete substrate, it can degrade the cementitious materials and alter the ITZ properties, making it difficult to achieve a strong bond between the new and old concrete layers.

Notably, there is a significant gap in the current literature regarding the influence of varying substrate surface roughness on reducing the detrimental effects of acidic solutions at this critical interface. Previous studies have broadly examined the effects of acidic solutions on concrete but have not explored how these solutions interact with the ITZ between old and new concrete when surface roughness varies. This lack of research presents a critical knowledge gap in understanding the durability of concrete repairs and overlays exposed to acidic environments. Therefore, the primary objectives of this study are to:

(1) Assess the durability of the bond between existing and new concrete in sulfuric acid, with a focus on how the roughness of the old concrete surface influences the bonding system's performance.
(2) Deliver essential data on the interactive effects of acid exposure and surface roughness on the long-term integrity of the ITZ through accelerated testing.

2. Materials and Methods

The properties of the constituent materials in the normal concrete mix are presented in Table 1. The concrete substrate and the new concrete overlay were both designed as normal-strength concrete with a target strength of approximately 30 MPa. Mix proportions for preparing specimens of the substrate and overlay are shown in Table 2.

The test specimens consisted of two congruent concrete layers: a normal-strength old concrete representing the existing substrate, and a repair layer of matching composition and grade (Fig. 1 and Table 3). These substrates were initially cast in lubricated molds and cured at room temperature for 24 hours, followed by demolding and a 28-day water cure. After this initial

curing period, the substrate surfaces were prepared using three roughening techniques: a control surface (CS), drilled holes surface (DS), and grooved surface (GS), as detailed in Fig. 2. After roughening, specimens were submerged in water for 24 hours, air-dried for approximately one hour before application of the new repair concrete layer. Finally, the two-layer specimens were demolded after 24 hours of curing at ambient temperature, then underwent an additional 28 days of water curing before being immersed in a sulfuric acid solution.

Table 1 Properties of raw materials for normal concrete

Properties	Cement	Fine aggregate	Coarse aggregate
Source	Ordinary Portland cement	Natural silica sand	Crushed limestone
Specific gravity (kg/m^3)	3.23	2.66	2.72
Specific surface area (cm^2/g)	2680	-	-
Soundness (mm)	1.5	-	-
Maximum grain size (mm)	-	2.7	19
Water absorption (%)	-	0.85	2.3
Fineness modulus	-	2.7	6.8

Table 2 Normal-strength concrete mix design

Items	Cement	Water	Fine aggregate	Coarse aggregate
Quantity (Kg/m^3)	390	180	420	1340

Table 3 Characteristics of the tested specimens

Specimen ID	Existing concrete (First layer)	Overlay concrete (Second layer)	Surface roughness technique
CS	Normal strength	Matching grade	As-cast
DS	Normal strength	Matching grade	Drilled holes
GS	Normal strength	Matching grade	Grooved surface

The concrete sulfate attack experiment utilized a (5% by volume) sulfuric acid solution in solution boxes [18]. The specimens, cured for 28 days, were submerged in the sulfate solution for 15 and 30 days, ensuring a minimum distance of 2 cm between specimens to maintain uniformity. Due to the rapid failure of CS (under 30 days), the sulfuric acid exposure test was limited to 30 days. A plastic film was applied to the sealed boxes to prevent evaporation. After exposure, the specimens were dried at room temperature for one day before bond strength testing. The sulfuric acid solution was replaced weekly, and the experiment was conducted at a controlled temperature of 25±2 °C.

(a) Slant shear specimens (b) Splitting tensile specimens (c) Testing machine

Fig. 1 Specimens and testing machine used in this study

The study included 54 specimens, which were divided into two main groups. The first group consisted of 27 specimens designated for split tensile strength testing. The second group also contained 27 specimens intended for slant shear testing. Each group was further subdivided into three sets of 9 specimens: 3 control specimens, 3 specimens tested after 15 days of immersion in an acidic solution, and 3 specimens tested after 30 days of immersion. Before conducting the slant shear test, ultrasonic pulse velocity (UPV) testing was performed on the slant shear specimens.

(a) Control surface (CS) (b) Drilled holes (DS) (c) Grooves (GS)

Fig. 2 Surface preparation

Slant shear specimens were prismatic, measuring 150 mm x 150 mm x 300 mm, with an interface line inclined at 30° to the vertical (Fig. 1(a) and Fig. 3). Compression testing followed ASTM C 882 standards, applying a constant loading rate of 0.50 MPa/s. Bond shear strength (f_s) can be obtained by:

$$f_s = \frac{P}{A} \tag{1}$$

where slant shear strength (MPa) equals the maximum force, P (N), divided by the slant surface area, A (mm²), approximated as (150 × 150) / sin 30°.

The tensile splitting test, conducted per ASTM C496 standards, assessed bond strength using cubic specimens measuring 150 mm × 150 mm × 150 mm (Fig. 1(b) and Fig. 4). This straightforward test yields more consistent results than other tension tests, with failure occurring due to indirect tension along the interfacial layer. A continuous loading rate of 0.05 MPa/s was applied. The splitting tensile strength (f_t) can be calculated assuming uniform tensile stress across the bond plane by:

$$f_t = \frac{2P}{\pi A} \tag{2}$$

where the applied force, P (N) is divided by the bonding surface area, A (mm²), and A ≈ 150 × 150 mm².

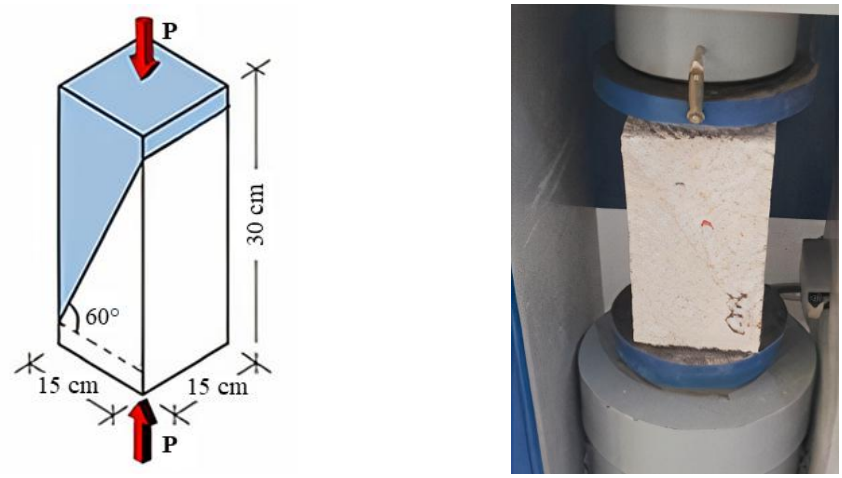

(a) Specimen dimension (b) Test setup

Fig. 3 Configurations of the slant shear test

ASTM C597-09 guided UPV testing assessed interfacial bond strength between existing and overlay concrete. UPV was directed parallel to the interface between the new and old concrete. Monitoring the velocity of these waves allows for the assessment of bond strength and the identification of voids or weak connections, particularly concerning the adverse effects of sulfuric acid on the studied surfaces.

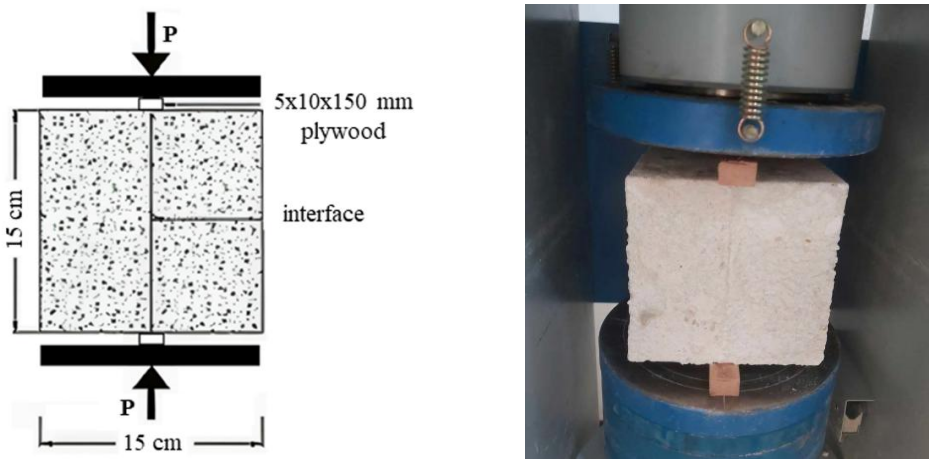

(a) Specimen dimension (b) Test setup

Fig. 4 Configurations of tensile splitting test

The effect of sulfuric acid on the bond is evaluated indirectly through phenolphthalein indicator testing after the splitting tensile test. The presence of a pink color (pH > 8.5) at the interface indicates minimal sulfuric acid influence due to concrete alkalinity. Conversely, colorless areas (pH < 8.5) suggest acid penetration and the formation of gypsum. Increased gypsum can exert pressure, causing debonding. This method indicates sulfuric acid ingress, even if gypsum formation is limited [19]. This approach aims to indicate the sulfuric acid's penetration, even if it does not directly contribute to gypsum formation. Understanding the extent of acid penetration allows for the evaluation of the effectiveness of different surface roughening techniques in preventing the acidic solution from penetrating. This assessment can help determine their impact on enhancing bond strength and interlocking between the old and new concrete layers.

In addition, powder specimens from the interface between new and existing concrete, obtained after sulfuric acid immersion and slant shear testing, were analyzed using X-ray diffraction (XRD) to identify the primary reaction phases. After immersion in sulfuric acid, 150 mm³ cubic specimens underwent mass loss testing. The total mass loss ML_t after 15 and 30 days can be calculated using the formula:

$$ML_t = \frac{M_t - M_i}{M_i} \tag{3}$$

where, M_t is the mass at time t (kg), and M_i is the initial mass (kg).

3. Results and Discussion

Table 4 and Fig. 5 present the results of the experimental slant shear strength tests, highlighting the significant impact of sulfuric acid solution. For each test, the coefficient of variation was calculated. The coefficient of variation, expressed as a percentage, is the standard deviation divided by the mean, providing a measure of relative variability. The coefficients of variation were found to be between 1.8% and 11.2%, consistently remaining below the 15% threshold. This low level of dispersion suggests a high degree of reliability in the test results. Furthermore, for CS, bond strength decreased by 73% after 15 days of immersion. Specimens immersed for 30 days failed before the testing period ended. In contrast, DS specimens showed a bond strength reduction of approximately 32% and 46% after 15 and 30 days, respectively. GS specimens experienced smaller reductions of around 10% and 24% during the same periods.

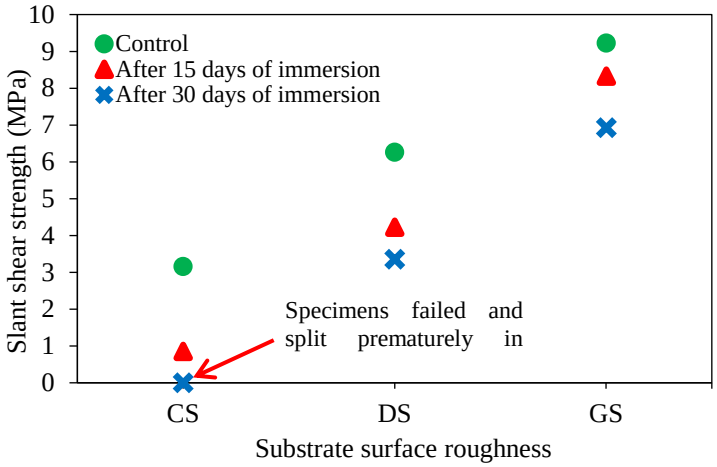

Fig. 5 Slant shear strength of specimens in acid solution at varying roughness levels

Notably, the GS demonstrated an increase in shear strength of 163% and 119% after 15 and 30 days of immersion compared to the CS. Additionally, the shear strength improvement for GS ranged from 41% to 17% relative to DS at corresponding intervals. These findings indicate that varying surface roughness profiles, such as DS and GS, significantly enhance the slant bond strength of the specimens compared to the non-roughened CS. The superior slant shear bond strength exhibited by rough surface treatments, particularly GS, can be attributed to enhanced interaction between the existing and newly placed concrete layers. The increased surface area and mechanical interlocking provided by the grooves help mitigate the effects of differential autogenous shrinkage between the two concrete layers, which can otherwise compromise the bond [20].

Table 4 Slant shear strength test results for various surface preparations

ID	Comp. strength (Control) (MPa)	Comp. strength at 15 d (MPa)	Comp. strength at 30 d (MPa)	Sla. shear strength (Control) (MPa)	CV (%)	Sla. shear strength at 15 d (MPa)	CV (%)	Sla. shear strength at 30 d (MPa)	CV (%)	Failure modes
CS	5.47	1.5	N/A	3.16	1.8%	0.86	11.2%	N/A	N/A	(A) at all testing dates
DS	10.9	7.4	5.9	6.26	3.6%	4.23	4.9%	3.36	10.3%	(B) at all testing dates except 30 days was (A)
GS	16.05	14.4	12.0	9.23	2.6%	8.33	4.8%	6.93	2.25%	(B) at all testing dates

CV: Coefficient of Variation, N/A: Results were unobtainable due to premature specimen failure.

The grooved surface topography creates a more tortuous path that obstructs the direct flow of the acidic solution, limiting its ability to penetrate and degrade the bond at the interface compared to smoother surface finishes [21]. This improved resistance to acid ingress, combined with the stress-distributing effect of the grooves, helps preserve the integrity of the ITZ between the existing and new concrete. In contrast, CS lack this enhanced bonding mechanism and are more vulnerable to the detrimental effects of the acidic environment [20]. These findings align with the guidance provided in ACI 546-23, which emphasizes the importance of adequate surface roughening to ensure durable and reliable concrete repair performance. Prior to sulfuric acid exposure, all specimens met the ACI Concrete Repair Guide (ACI 364.1R-19) minimum slant shear strength (6.9–12 MPa). Post-immersion, only GS specimens consistently maintained this strength.

The failure patterns can be categorized into four distinct types. Type A represents a pure interfacial failure, where separation occurs exclusively along the interface region between materials. Type B exhibits a mixed failure mode, with separation at the interface accompanied by detachment of the substrate material. In Type C failures, interfacial separation is

coupled with substrate fracture. Finally, Type D failures involve substratum failure while maintaining a robust interface bond [4, 22]. The slant shear composite specimens exhibited two distinct failure modes upon testing, as illustrated in Fig. 6.

Type A failure was characterized by complete interfacial debonding at the transition zone, while Type B involved interfacial failure along with substrate cracking or minor damage. Notably, the CS surface consistently displayed Type A failure behavior, both before and after immersion in sulfuric acid, which corresponds to the lowest recorded shear bond strength due to insufficient substrate preparation. In contrast, the majority of failure modes for DS and GS surfaces were Type B, although DS specimens exhibited Type A failure after 30 days of sulfuric acid exposure. This mixed-mode failure, featuring partial substrate failure, correlates with the higher bond strengths observed for these treated surfaces, indicating improved interfacial adhesion. The varying surface roughness treatments significantly influenced the observed failure mechanisms, which correlated with the measured slant bond strengths. Specifically, the GS surface demonstrated the maximum slant bond strength, consistent with the Type B failure mode characterized by interface failure and partial substrate failure.

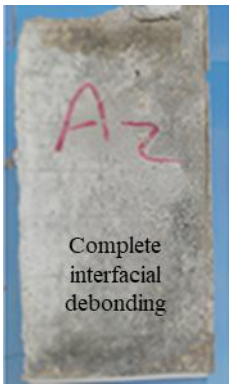

(a) CS-type A failure (0 & 15 days)

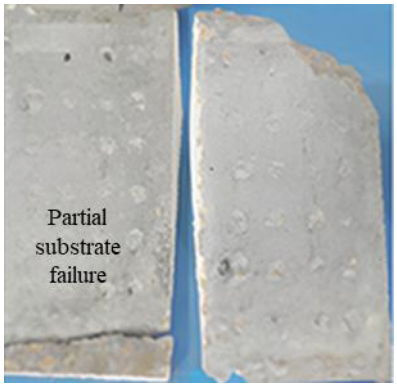

(b) DS-type B failure (15 days)

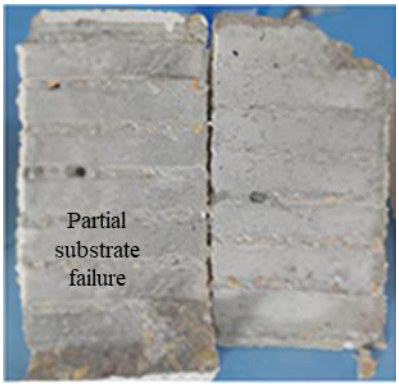

(c) GS-type B failure (30 days)

Fig. 6 Typical failure modes of slant shear specimens

The trend observed for shear strength is similarly reflected in the impact of surface roughness on compressive strength (Table 4). Specimens with grooved surfaces exhibited the highest compressive strength values, followed by those with drilled surfaces. This pattern held regardless of whether the specimens were immersed in sulfuric acid solution for 15 or 30 days. This is consistent with the findings of Diab et al. [20], who reported that an increase in concrete compressive strength leads to a corresponding increase in the slant shear bond strength between old concrete and new self-compacting concrete. The parallelism between the effects on shear and compressive strength underscores the significance of surface texture in influencing a material's resistance to both shear and compressive forces in corrosive environments. According to Altwair et al. [6], surface roughness, with a focus on GS, is highly effective in boosting the bond durability between old and new concrete. The study found that GS significantly improved slant shear bond strength, with increases of 81% and 90% after 30 and 60 days in a NaCl solution, when compared to CS.

Indirect tensile strength was assessed using splitting tensile testing, with results presented in Table 5 and Fig. 7. The slant splitting tensile test results exhibited coefficients of variation ranging from 2.3% to 13.3%. This limited variability signifies low dispersion, implying that the obtained results are highly reliable. All modified substrate surfaces displayed a substantial increase in splitting tensile capacity compared to control specimens prior to acid immersion. The recorded tensile strengths ranked as follows: CS, DS, and GS, aligning with trends observed in slant shear strength tests.

Table 5 Results of splitting tensile test conducted on various surface treatments

ID	Split tensile strength (Control) (MPa)	CV (%)	Split tensile strength at 15 d (MPa)	CV (%)	Split tensile strength at 30 d (MPa)	CV (%)	Failure modes
CS	3.8	2.6%	N/A	N/A	N/A	N/A	N/A
DS	4.59	8.6%	3.1	2.3%	2.29	13.3%	(A) at all testing dates
GS	5.17	6.1%	3.15	4.2%	2.75	4.5%	(B) at all testing dates except 30 days was (A)

CV: Coefficient of Variation, N/A: Results were unobtainable due to premature specimen failure.

Notably, the CS specimens failed, with separation of the overlay and substrate concrete occurring in the acid solution before evaluation. Despite a reduction in tensile strength, the DS and GS specimens demonstrated notable durability against acid exposure. The GS specimens achieved the highest tensile strength values after 15 and 30 days of immersion, showing increases of 1.6% and 17%, respectively, compared to the DS specimens. Thus, the grooved surface preparation technique is confirmed as the most effective method, yielding superior splitting tensile capacity relative to the other techniques employed.

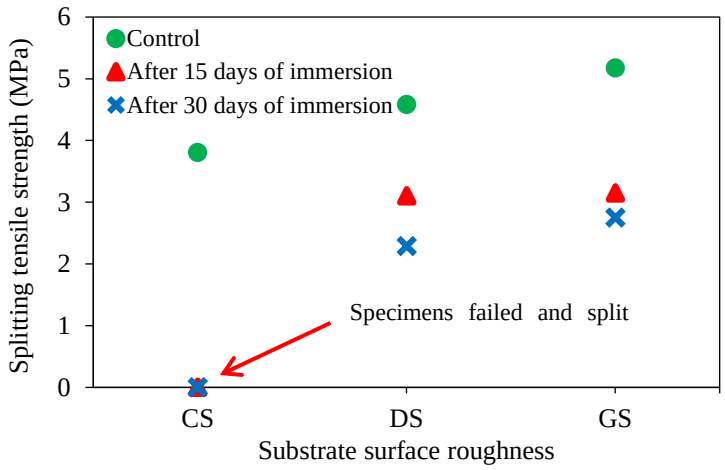

Fig. 7 Splitting tensile strength of specimens in acid solution at varying roughness levels

The presence of surface grooves on old concrete can significantly improve the bond strength with new concrete overlays. This enhancement is attributed to several factors. Firstly, the grooved geometry provides an interlocking mechanism that enhances the mechanical connection between the layers, effectively preventing slippage at the interface [20]. Secondly, the increased surface area facilitated by the grooves promotes improved chemical adhesion and mechanical interlocking between the old and new concrete. Additionally, the grooved surface creates a keying effect, which distributes stresses more evenly between the two concrete layers, reducing the likelihood of cracks or debonding. Lastly, the rough, grooved surface helps to distribute stresses more uniformly, minimizing stress concentrations and potential failure points [23].

Furthermore, there is an inverse correlation between the concrete's splitting tensile strength and the penetration of sulfuric acid solution. Higher tensile strength indicates stronger cohesion and bonding between the concrete layers, which impedes the acid solution from infiltrating the interface [20]. This principle elucidates the observed behavior of DS and GS specimens subjected to sulfuric acid exposure, where the interfacial transition zone with greater tensile strength exhibits reduced acid penetration.

The failure modes observed in the rough specimens following the splitting tensile test are illustrated in Fig. 8. All drilled hole specimens DS exhibited failure mode A, while the grooved surfaces displayed failure mode B, characterized by the failure of the underlying concrete substrate. The enhanced strength of the grooved surfaces is attributed to improved interfacial bonding, which effectively shifts the failure point outside the bonding region at the interface between the substrate and overlay concrete. Additionally, Bond quality can be categorized into five levels based on bond strength: excellent (> 2.1 MPa), very good (1.7-2.1 MPa), good (1.4-1.7 MPa), fair (0.7-1.4 MPa), and poor (0-0.7 MPa) [24]. The DS and GS substrates both demonstrate exceptional bond strength, with measured values surpassing 2.1 MPa.

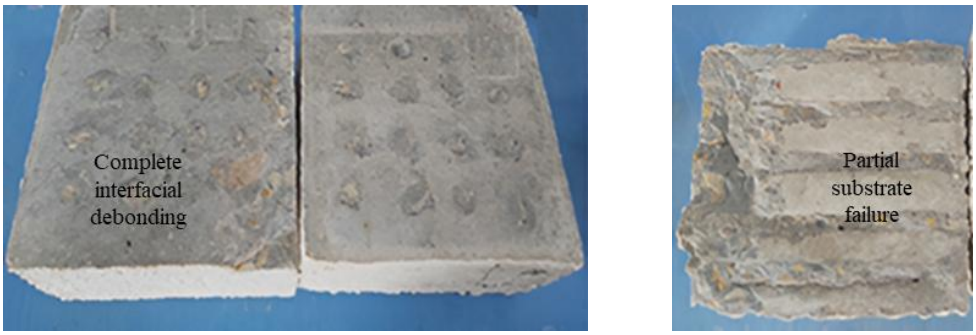

(a) DS-type A failure (15 days) (b) GS-type B failure (30 days)

Fig. 8 Typical failure modes of splitting tensile specimens

This enhancement stems from increased mechanical interlocking due to groove geometry and increased surface area for mechanical and chemical bonding. The grooves create a keying effect, distributing stresses between old and new concrete and reducing the likelihood of cracking or debonding. The grooved surface promotes uniform stress distribution, minimizing stress concentrations and potential failure points [23]. Moreover, the results related to the effect of the surface roughness were found to be in good agreement with those of Altwair and Jarir. [4], who found that the higher splitting strength of the grooved surfaces is justified by their superior interfacial bond.

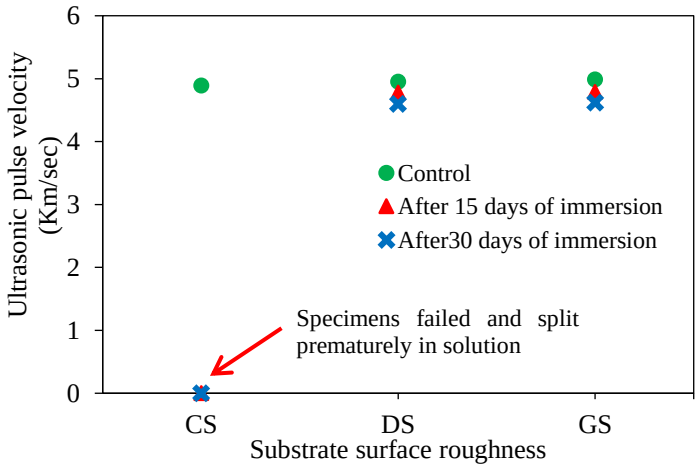

Fig. 9 UPV of specimens in sulfuric acid at varying roughness after 15 and 30 days

According to Shawafi et al. [25], an investigation into the bond behavior of normal concrete (NC), ultra-high-performance concrete (UHPC), and polyurethane-based polymer concrete (PUC) under various loading conditions revealed that surface roughness plays a crucial role. The study emphasized that the grooved surface treatment enhanced splitting tensile bond strength, with the NC-PUC interface showing a 15.7% higher strength than the NC-UHPC interface when the GB surface was used. However, the unique resistance of grooved surfaces to sulfuric acid is likely due to the complex, interlocking surface profile. This increased roughness enhances mechanical interlocking, increasing frictional resistance against separation [26]. The larger bonding interface created by the grooves compensates for potential weakening of cement paste and chemical bonds caused by the acidic solution [6], improving overall bond strength and resistance to delamination.

The effect of sulfuric acid exposure on the UPV of specimens with varying surface preparation methods, following 15 and 30 days of immersion, is depicted in Fig. 9. Prior to acid solution immersion, the UPV for CS, DS, and GS specimens were 4.89 km/s, 4.95 km/s, and 4.99 km/s, respectively, with negligible differences among the standard specimens. However, the GS specimen exhibited a slight increase. After being submerged in the acid solution for 15 and 30 days, no significant distinctions in UPV were observed between DS and GS specimens immersed in the acid solution, except for CS specimens that had already failed before evaluation.

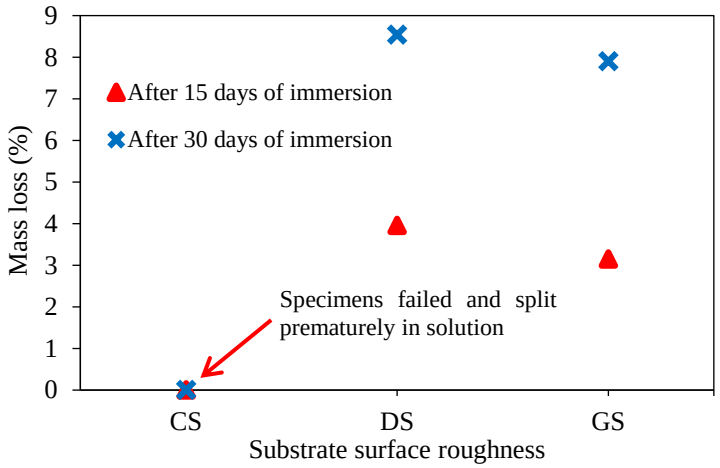

Fig. 10 Mass lost at 15 and 30 days after being exposed to a 5% sulfuric acid solution

This consistency suggests that the acid solution primarily affected the specimens' exterior surfaces, leaving the substrate-overlay concrete interface zone unaltered. The minimal UPV reduction for DS and GS specimens implies that the acid solution did not weaken the bonding effectiveness resulting from the surface roughening technique. By eliminating potential weak planes at the interface zone, roughening the existing concrete surface enhances bonding. This outcome indicates that the interface zone remains unaffected by the acid solution, further supporting the effectiveness of the surface preparation methods in maintaining bond strength and durability. Surface roughening techniques improve interfacial bond strength in composite systems by reducing weak points and enhancing load transfer. Roughened surfaces allow fresh concrete to fill voids, ensuring uniform contact with the existing substrate, strengthening mechanical interlocking and chemical bonding. This optimizes stress transfer and maintains high UPV, indicating strong bond strength and minimal weak points in the interface zone [27].

(a) CS-completely split (5 days) (b) DS/GS-increased aggregate exposure (7 days)

Fig. 11 Specimens submerged in the 5% sulfuric acid solution

This study's results regarding the effect of substrate surface roughness on UPV align with the findings of Fan et al. [27], who demonstrated that increased roughness of aged concrete surfaces positively correlates with enhanced UPV due to the mechanical interlocking forces created by the surface roughness. Furthermore, Santos et al. [28] explored using UPV methods

to assess the surface roughness of aged concrete after applying a new layer. Their numerical studies showed that exciting the concrete with UPV allows identification of generated pulses, confirming that pulse velocity at the interface correlates with surface roughness at 500 kHz.

The mass loss of specimens immersed in a 5% sulfuric acid solution over 15 and 30 days is illustrated in Fig. 10. After 15 days, the dry surface DS specimens exhibited a mass loss of 3.96%, while the GS specimens showed a loss of 3.15%. Upon further immersion for 30 days, the mass loss increased to 8.54% for DS and 7.90% for GS. Notably, despite the identical volumes of DS and GS specimens, the GS specimens consistently demonstrated lower mass loss compared to DS specimens. This suggests that DS specimens are more susceptible to degradation by sulfuric acid, potentially due to acid penetration into the bonding zone between the new concrete and the existing substrate, leading to mass reduction in affected areas.

The findings indicate that the method employed for surface preparation significantly influences concrete behavior in acidic environments. Moreover, the separation observed between the new concrete and the existing substrate with the concrete substrate CS may stem from weak bond strength. Additionally, tensile forces resulting from corrosion product accumulation can exacerbate this separation, as the expansion of these products may induce cracking in the contact area, ultimately resulting in premature failure [29].

Upon immersion in the solution, the acid immediately initiated a reaction with the specimens, evident by the ascent of air bubbles to the surface of the solution. Indeed, sulfuric acid will chemically react with the compounds formed during the process of cement hydration, resulting in the formation of soluble reaction products. These reaction products will then be removed from the surface of the concrete. The $Ca(OH)_2$ phase, which is more abundant, is more vulnerable to the sulfate ions present in sulfuric acid. As a result, this reaction leads to the formation of white, expanding gypsum components that are apparent on the surface of the specimens [26].

From the first day of exposure, a white powdery substance (specifically recognized as gypsum) gradually accumulated on the surface of all specimens, without any significant variations seen among them. The continuous extraction of gypsum resulted in an off-white residue at the bottom of containers, resembling the consistency of freshly mixed cement paste. Following three days of immersion, the CS specimens started debonding. After 5 days, all of the CS specimens split (Fig. 11(a)). By the end of the first week of immersion, the DS and GS specimens displayed exposed aggregates. As the acidic reactions continued, the aggregates were much more exposed (Fig. 11(b)).

Premature failure | At 15 days | At 30 days | At 15 days | At 30 days

(a) Control surface | (b) Drilled holes surface | (c) Grooved surface

Fig. 12 Visualizing sulfuric acid attack on surface roughness with phenolphthalein

Fig. 12 illustrates the visual appearance of CS, DS, and GS surfaces after being exposed for 15 and 30 days to the 5% sulfuric acid solutions. The photograph depicts that gypsum has accumulated on the previously split surfaces of the CS. The findings indicate that the acidic solution had a substantial effect on this particular type of bonding. As a result, the overlay concrete and the existing concrete substrata broke apart before the time limit for testing the bond strength was up (Fig. 12(a)).

As mentioned before, the presence of a pink color in concrete implies a pH level higher than 8.5 and alkalinity. The colorless areas normally signify a lower pH of less than 8 and the presence of products formed from reactions with chemical solutions. However, the color did not transition to pink while spraying the phenolphthalein solution onto the CS surface,

indicating a decreased pH level. Furthermore, there was no obvious effect of the acid solution on the DS specimens even after a 15-day exposure period. Although some regions of the specimen, with a depth not exceeding 1 cm, experienced a fading to a pink color, the bright pink color was noticed uniformly over the whole surface area of the DS specimens. Indicating that the pH level exceeds 8.5. A slight decrease in the intensity of the pink color was observed in the DS specimens after 30 days of immersion. This observation suggests that the acidic solution had a negligible impact on the interfacial transition zone between the old and new concrete layers, suggesting that the pH remained above 8.5 (Fig. 12(b)).

Considering the GS specimens, it is noted that the GS was not affected by the acidic solution, whether after 15 or 30 days of immersion in the acidic solution, and this is evident in the photograph shown in Fig. 12(c). It can be observed that no colorless zones can be spotted on any of the specimens, and only a bright pink color is noticed. This validates what was previously addressed in the instance of analyzing the findings of bond strength testing.

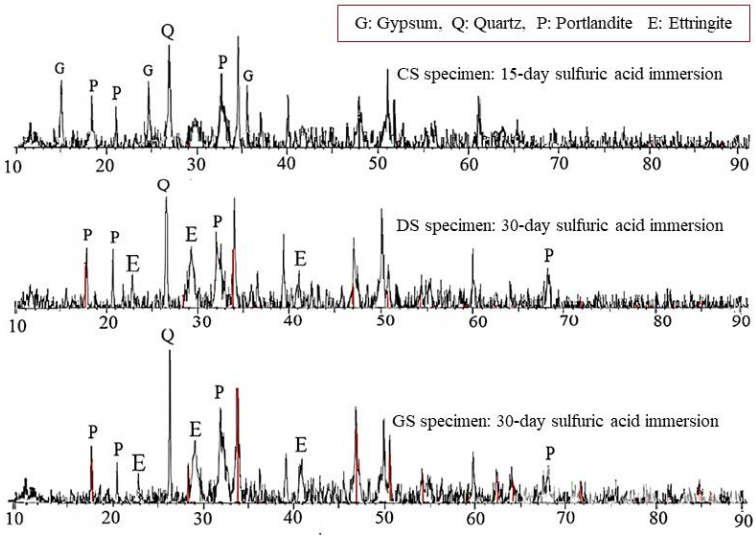

Fig. 13 XRD patterns of specimens with varying roughness in acid solution

The XRD results shown in Fig. 13 indicate that, despite the 15-day sulfuric acid immersion period for the CS specimens compared to the DS and GS specimens, the formation of gypsum ($CaSO_4 \cdot 2H_2O$) was evident at the interface between the new and existing concrete for the CS specimens. This suggests that the sulfuric acid solution was able to penetrate the interfacial surface of the CS, leading to a reaction with the hydration products and subsequent gypsum formation [30]. However, the lack of ettringite formation was observed, likely due to the low pH conditions. The formation of gypsum can be represented by:

$$Ca(OH)2 + H2SO4 \rightarrow CaSO4 \cdot 2H2O \text{ (Gypsum formation)} \quad (4)$$

In contrast, the DS and GS specimens, which were immersed in the acidic solution for 30 days, did not exhibit gypsum formation at the interface zone. Instead, the formation of ettringite and the presence of quartz (from the sand) along with abundant portlandite were observed. The absence of gypsum in the interfacial zone for the DS and GS specimens suggests that the acid solution was unable to penetrate the surface due to the improved bond resistance provided by the roughened surface.

4. Conclusions

This study investigates the effects of surface roughness on bond strength and durability of concrete under sulfuric acid exposure, highlighting significant improvements with grooved and drilled hole surface treatments. The obtained results of experimental verification allow drawing the following conclusions:

(1) GS significantly enhanced shear strength, showing up to 163% improvement over CS after immersion in a 5% sulfuric acid solution. This aligns with ACI 546-23 guidance, emphasizing surface roughening for durable concrete repair.

(2) The slant shear test revealed CS consistently displayed Type A (interfacial) failure, whereas GS and DS surfaces exhibited Type B (substrate failure), correlating with increased bond strengths and enhanced interfacial adhesion.

(3) The study found that surface preparation significantly impacted tensile strength. The CS specimens failed, while the GS and DS specimens exhibited higher tensile strength, even after acid exposure. GS specimens showed the highest tensile strength, with a 17% increase after 30 days of immersion compared to DS.

(4) Bond quality for both GS and DS exceeded 2.1 MPa, classified as excellent, due to enhanced mechanical interlocking and increased surface area. Failure modes shifted from interface failure (Mode A) in DS specimens to substrate failure (Mode B) in GS, indicating stronger interfacial bonding and uniform stress distribution.

(5) The sulfuric acid solution did not significantly affect the UPV of specimens. The roughened surfaces improved the contact area and load transfer mechanism, sustaining higher UPV values.

(6) Excluding the failed CS specimens, DS specimens showed a slightly higher mass loss compared to GS specimens when exposed to 5% sulfuric acid for 15 and 30 days, indicating varied performance under acidic conditions.

(7) After five days in 5% sulfuric acid, CS specimens experienced complete debonding and splitting. DS and GS specimens showed aggregate exposure, but GS specimens maintained integrity, exhibiting no significant changes in pH levels after 30 days.

(8) XRD results show gypsum formation at CS interfaces due to acid penetration, while roughened DS and GS surfaces resist acid penetration, forming ettringite instead, indicating better acid resistance.

The study demonstrates that creating grooves on concrete surfaces is the most effective technique for durable repairs. Implementation involves cleaning the surface, employing methods like diamond saw cutting to create engineered grooves, where deeper grooves optimize mechanical interlocking and closer spacing maximizes bonding. A final cleaning ensures an optimal substrate. This comprehensive approach yields robust, long-lasting repairs. Future research should explore surface treatments like steel brushing and blasting to enhance sulfuric acid resistance. Combining these with advanced materials and monitoring technologies can enable real-time performance assessments. Further investigation into the economic and practical implications of each technique is essential, including a cost-benefit analysis.

Abbreviations and Symbols

CS	Control surface (As-cast surface)		M_t	Mass at time (t)
DS	Drilled holes surface		M_i	Initial mass
GS	Grooved surface		f_t	Splitting tensile strength
ITZ	Interfacial Transition Zone		f_s	Bond shear strength
XRD	X-ray Diffraction		ph	Potential of hydrogen
CV	Coefficient of Variation		UPV	Ultrasonic Pulse Velocity
ML_t	Total mass loss		UHPC	Ultra-High Performance Concrete
NC	Normal Concrete		PUC	Polyurethane-Based Polymer Concrete

Conflicts of Interest

The authors declare no conflict of interest.

References

[1] G. Zhang and Y. Lu, “Quantifying Anisotropic Properties of Old–New Concrete Interfaces Using X-Ray Computed Tomography and Homogenization,” Infrastructures, vol. 10, no. 1, article no. 20, 2025.

[2] A. Suzuki, et al., “Structural Damage Detection Technique of Secondary Building Components Using Piezoelectric Sensors,” Buildings, vol. 13, no. 9, article no. 2368, 2023

[3] K. Belmokretar, K. Ayed, D. E. Kerdal, N. Leklou, and M. Mouli, "New Repair Material for Ordinary Concrete Substrates: Investigating Self-Compacting Sand Concrete and Its Interaction with Roughness of the Substrate Surface," Journal of Materials in Civil Engineering, vol. 35, no. 9, 2023.

[4] N. M. Altwair and S. J. Jarir, "Influence of Surface Roughness on Adhesion Between the Existing and New Plain Concretes," Proceedings of First Conference for Engineering Sciences and Technology, vol. 2, pp. 581-591, 2018.

[5] S. Mokhtari and M. Hassan, "Performance of Bond between Old and New Concrete Layers: The Effective Factors, Durability and Measurement Tests—A Review," Infrastructures, vol. 9, no. 10, article no. 171, 2024.

[6] N. N. M. Altwair, N. Y. O. Yacoub, N. A. M. Alsharif, and N. L. S. Sryh, "Influence of Surface Roughness on Durability of New-Old Concrete Interface," Advances in Technology Innovation, vol. 9, no. 2, pp. 143–155, 2024.

[7] D. Daneshvar, A. Behnood, and A. Robisson, "Interfacial Bond in Concrete-to-Concrete Composites: A Review," Construction and Building Materials, vol. 359, article no. 129195, 2022.

[8] G. Li, H. Hu, and C. Ren, "Resistance of Segmental Joints to Chloride Ions," ACI Materials Journal, vol. 113, no. 4, 2016.

[9] F. Li and X. Luo, "Interfacial Zone Effects of Chloride Penetration in Precast Concrete Member Joints," Advances in Cement Research, vol. 31, no. 6, pp. 279–289, 2018.

[10] R. Qin, H. Hao, T. Rousakis, and D. Lau, "Effect of Shrinkage Reducing Admixture on New-to-Old Concrete Interface," Composites Part B: Engineering, vol. 167, pp. 346–355, 2018.

[11] J. Zhao and F. Li, "Chloride Transport in Interfacial Zone of New–Old Concrete Joints of Precast Prestressed Concrete Bridges under Fatigue Load," Journal of Materials in Civil Engineering, vol. 34, no. 10, 2022.

[12] J. Xia, et al., "Experimental and Numerical Study on the Microstructure and Chloride Ion Transport Behavior of Concrete-to-Concrete Interface," Construction and Building Materials, vol. 367, article no. 130317, 2023.

[13] J. Zhang, Y. Pan, J. Li, H. Yun, and Z. Guan, "Experimental Study on Chloride Penetration of the New-to-Old Concrete Interface," Construction and Building Materials, vol. 420, article no. 135585, 2024.

[14] S. Gao, J. Jin, G. Hu, and L. Qi, "Experimental Investigation of the Interface Bond Properties Between SHCC and Concrete under Sulfate Attack," Construction and Building Materials, vol. 217, pp. 651–663, 2019.

[15] G. Li, H. Hu, and C. Ren, "Resistance of Segmental Joints to Carbonation," ACI Materials Journal, vol. 114, no. 1, pp. 137-148, 2017.

[16] C. Yi, et al., "Freeze-Thawing Damage Model of New-to-Old Concrete with Different Rough Interfaces," Applied Mechanics and Materials, vol. 405–408, pp. 2707–2714, 2013.

[17] S. A. Hadigheh, R. J. Gravina, and S. T. Smith, "Effect of Acid Attack on FRP-to-Concrete Bonded Interfaces," Construction and Building Materials, vol. 152, pp. 285–303, 2017.

[18] A. M. Ibrahim, M. T. Bassuoni, J. Carroll, and A. Ghazy, "Performance of Concrete Superficially Treated with Nano-Modified Coatings under Sulfuric Acid Exposures," Journal of Building Engineering, vol. 86, article no. 108957, 2024.

[19] Y. Sumra, S. Payam, and I. Zainah, "The pH of Cement-Based Materials: A Review," Journal of Wuhan University of Technology-Materials Science Edition, vol. 35, no. 5, pp. 908–924, 2020.

[20] A. M. Diab, A. E. M. A. Elmoaty, and M. R. T. Eldin, "Slant Shear Bond Strength Between Self Compacting Concrete and Old Concrete," Construction and Building Materials, vol. 130, pp. 73–82, 2017.

[21] B. Zhang, et al., "Interface Shear Failure Behavior Between Normal Concrete (NC) and Ultra-High Performance Concrete (UHPC)," International Journal of Concrete Structures and Materials, vol. 18, article no. 18, 2024.

[22] V. B. dos Santos, et al., "Influence of Wetting Conditions and Concrete Strength of Both Substrate and Repair Material on the Bond Capacity of Repaired Joints," Buildings, vol. 13, no. 3, article no. 643, 2023.

[23] Y. Wang, X. Jiang, K. Li, and J. Qiang, "Experimental Study of Interfacial Adhesion Performance of Prefabricated UHPC-NC Diagonal Shear Groove," Case Studies in Construction Materials, vol. 19, article no. e02343, 2023.

[24] A. Kuncoro, et al., "Evaluation of Bonding Performance of Ultra High-Performance Concrete with Fly Ash Content as Overlay on Normal Strength Concrete," IOP Conference Series: Earth and Environmental Science, vol. 1195, no. 1, article no. 012020, 2023.

[25] A. Al-Shawafi et al., "Bond Behavior Between Normal Concrete and UHPC and PUC Layers Subjected to Different Loading Conditions Coupled with Fracture Analysis Technique," Journal of Building Engineering, vol. 86, article no. 108880, 2024.

[26] Q. Dong, Y. Li, J. Wei, and F. Lu, "Layered Structures with Rough Surfaces and Interfaces at Contact Loading," International Journal of Mechanical Sciences, vol. 178, article no. 105611, 2020.

[27] J. Fan, L. Wu, and B. Zhang, "Influence of Old Concrete Age, Interface Roughness and Freeze-Thawing Attack on New-to-Old Concrete Structure," Materials, vol. 14, no. 5, article no. 1057, 2021.

[28] P. Santos, E. Júlio, and J. Santos, "Towards the Development of an In Situ Non-Destructive Method to Control the Quality of Concrete-to-Concrete Interfaces," Engineering Structures, vol. 32, no. 1, pp. 207–217, 2010.

[29] J. Xiao et al., "Experimental Study on the Sulfuric Acid Corrosion Resistance of PHC Used for Pipe Pile and NSC Used in Engineering," Buildings, vol. 13, no. 7, article no. 1596, 2023.

[30] N. Djerfaf, Z. Nafa, and A. S. E. Belaidi, "Durability of High-Performance Concrete to an Attack by a Mixture of Sulfuric Acid and Acetic Acid," Epitoanyag-Journal of Silicate Based and Composite Materials, vol. 75, no. 1, 2023.